

Hypothermia preconditioning improves cardiac contractility after cardiopulmonary resuscitation through AMPK-activated mitophagy

Yuanzheng Lu^{1,2}, Chenyu Zhang¹, Jie Chen³, Qiuping Zou⁴, Bo Li², Hongyan Wei¹, Mary P Chang⁵, Xiaoxing Liao^{2,6} and Chunlin Hu¹ 

¹Department of Emergency Medicine, The First Affiliated Hospital, Sun Yat-sen University, Guangzhou 510080, P.R. China;

²Department of Emergency Medicine, The Seventh Affiliated Hospital, Sun Yat-sen University, Shenzhen 518107, P.R. China;

³Department of Critical Care Medicine, The First People's Hospital of Dongguan, Dongguan 523059, P.R. China; ⁴Department of Emergency Medicine, The First People's Hospital of Dongguan, Dongguan 523059, P.R. China; ⁵Department of Emergency Medicine, University of Texas at Southwestern Medical Centre, Dallas, TX 75390, USA; ⁶Research Institute, Sun Yat-sen University, Shenzhen 518057, P.R. China

Corresponding authors: Chunlin Hu. Email: huchunl@mail.sysu.edu.cn; Xiaoxing Liao. Email: liaowens@163.com

Impact Statement

We investigated the potential molecular mechanisms leading to the cardiac protection of Hypothermia Preconditioning (HPC). We found that the activity of adenosine monophosphate protein kinase (AMPK) in the heart of rats was significantly increased by HPC, which was accompanied by increased messenger RNA abundance, protein contents, and activities of ULK1 and mitophagy factors. Moreover, HPC increased autophagic flux in both *vivo* and *vitro*. Suppression of AMPK by Compound C in cultured cardiomyocytes attenuated the myocardial protection by HPC. In conclusion, we demonstrated both *in vitro* and *in vivo* that HPC provides cardioprotection after cardiac arrest (CA)/cardiopulmonary resuscitation (CPR) and return of spontaneous circulation (ROSC), at least in part through AMPK-activated mitophagy.

Abstract

Hypothermia preconditioning (HPC) improves cardiac function after cardiac arrest, yet the mechanism is unclear. We hypothesized that HPC-activated adenosine monophosphate-activated protein kinase (AMPK) activity may be involved. Adult male Wistar rats were randomly divided into normothermia Control, HPC (cooling to 32–34°C for 30 min), and HPC + Compound C (Compound C 10 mg/kg was injected intraperitoneally 30 min before HPC group). The rats underwent 7 min of untreated ventricular fibrillation (VF) followed by cardiopulmonary resuscitation (CPR). Cardiac function and hemodynamic parameters were evaluated at 4 h after return of spontaneous circulation (ROSC). Survival status was determined 72 h after ROSC. Mechanistically, we further examined the AMPK-Unc-51 Like Autophagy Activating Kinase 1 (ULK1)-mitophagy pathway and autophagic flux *in vivo* and *in vitro*. Six of twelve rats in the Control group, 10 of 12 rats in the HPC group, and 7 of 12 rats in HPC + Compound C group were successfully resuscitated. The 72-h survival rates were 1 of 12 Control, 6 of 12 HPC, and 2 of 12 HPC + Compound C rats, respectively ($P=0.043$). Rats in the HPC group demonstrated greater cardiac contractility and hemodynamic stability which were compromised by Compound C. Furthermore, HPC increased the protein levels of p-AMPK α and p-ULK1 and promoted the expression of mitochondrial autophagy-related genes. Compound C decreased the expression of mitochondrial autophagy-related genes and reduced

autophagic flux. Consistent with the observations obtained *in vivo*, *in vitro* experiments in cultured neonatal rat cardiomyocytes (CMs) demonstrated that HPC attenuated simulated ischemia–reperfusion-induced CM death, accompanied by increased AMPK-ULK1-mitophagy pathway activity. These findings suggest that AMPK-ULK1-mitophagy pathway was activated by HPC and has a crucial role in cardioprotection during cardiac arrest. Manipulation of mitophagy by hypothermia may merit further investigation as a novel strategy to prevent cardiac ischemia–reperfusion injury.

Keywords: Cardiac arrest, hypothermia preconditioning, cardiac dysfunction, AMPK-induced mitophagy

Experimental Biology and Medicine 2022; 247: 1277–1286. DOI: 10.1177/15353702221081546

Introduction

Postresuscitation myocardial dysfunction is a frequent and fatal complication, which accounts for 31% of deaths after cardiopulmonary resuscitation (CPR), where the deteriorating hemodynamic instability leads to multiple organ failure (MOF) and cardiovascular events.¹ Improvement in cardiac dysfunction during the early stages after return of spontaneous circulation (ROSC) increases survival rate of cardiac arrest (CA) patients.² Therefore, efforts should be focused on improving cardiac dysfunction in the early phase after CA.

Currently, there is no satisfactory cardioprotective treatment for patients suffering from myocardial ischemia–reperfusion (I/R) injury. Although therapeutic hypothermia management (TTM) is recommended to improve neurological outcome after CA, its impact on cardiac function is still controversial.^{3–7} Degradation of mitochondrial quality can cause postresuscitation myocardial dysfunction during I/R process by reactive oxygen species (ROS) production and cell death pathway activation. Accordingly, the timely removal of damaged mitochondria via mitophagy is critical for CM (cardiomyocyte) homeostasis and function.^{8,9} In our previous study, we found that hypothermia preconditioning (HPC) could mitigate cardiac dysfunction after CA by attenuating myocardial mitochondrial injury, but the underlying molecular mechanism was not yet elucidated.¹⁰

The adenosine monophosphate-activated protein kinase (AMPK) is a key regulator of cellular and whole-body energy homeostasis. In cardiovascular tissue, its specific role is to regulate cardiac metabolism and contractility, anti-inflammatory, and antiatherogenic actions.¹¹ Recent evidence shows that AMPK-dependent phosphorylation of Unc-51 Like Autophagy Activating Kinase 1 (ULK1) is critical for mitophagy in response to hypoxic stress.¹² Given the findings above, we hypothesize that AMPK may play an important role in HPC-regulated myocardial mitophagy after CA. We addressed our hypothesis in a rat CA model and in cultured CMs subjected to oxygenation deprivation and reoxygenation to simulate I/R.

Materials and methods

Animals

This experiment was approved by the Animal Ethics Committee of Sun Yat-sen University (protocol no. [2013] A-067). Animal care was in accordance with the recommendations of Guidelines for the Care and Use of Laboratory Animals formulated by the National Research Council. Healthy adult male Wistar rats, weighing 380–400 g, were provided by the Experimental Animal Center of Sun Yat-sen University. Animals were kept in a specific-pathogen-free room for one week and were fasted the night before the experiment.

Antibodies

Antibodies against AMPK α (2532), Phospho-AMPK α (Thr172) (40H9) (2535), Phospho-ULK1 (Ser757) (D7O6U) (14202), ULK1 (D8H5) (8054), Akt (2920), and Phospho-(Ser/Thr) Akt (9611) were purchased from Cell Signaling Technology (Danvers, MA, USA). Anti-light chain 3 (LC3) A/B (ab128025), -Atg5 (2630), and -Atg7 antibodies (2631)

were bought from Abcam (Cambridge, UK). Glyceraldehyde 3-phosphate dehydrogenase (GAPDH) monoclonal antibody was purchased from Proteintech (Rosemont, IL, USA). Goat antirabbit IgG (sc-2004) secondary antibody was purchased from Santa Cruz Biotechnology (Dallas, TX, USA). Rabbit antimouse IgG (A9044) secondary antibody was purchased from Sigma (St. Louis, MO, USA). Goat antimouse IgG (DyLight™ 488 conjugated) (#4316) secondary antibody was obtained from Cell Signaling Technology.

Procedures

Pentobarbital sodium 30 mg/kg was injected intraperitoneally (i.p.), followed by 1/4 of the initial dose for maintenance as needed. After anesthesia was established, the animal was secured on the experimental table, intubated with a 14 G sheath, and connected to the small animal ventilator. The ventilation frequency was 75 times/min and the tidal volume was 15 mL/kg. Lead II electrocardiogram was monitored continuously. The femoral artery and vein were punctured with 24 G indwelling needle and tubes were inserted for arterial blood pressure monitoring and intravenous drug delivery, respectively. An electric blanket was adjusted to keep the rectal temperature at $37 \pm 0.5^\circ\text{C}$. A 4F central venous catheter was inserted via the left carotid artery and advanced into the left ventricle (LV) to record left ventricular end systolic pressure (LVESP), left ventricular end diastolic pressure (LVEDP), left ventricular dp/dt_{\max} and dp/dt_{\min} values, and cardiac output (CO) before CA, and at 60, 120, 180, and 240 min after ROSC. All the data were recorded using a data acquisition (modelMP150, version3.8.1; BIOPACMP150, Goleta, CA, USA).

Ventricular fibrillation model

The induction of ventricular fibrillation (VF) has been described in our previous publications.^{10,13} Two acupuncture needles were inserted transcutaneously into the epicardium between the fourth rib of the left sternal border and the third rib of the right sternal border. VF was induced by an external transthoracic alternating current (50 Hz, 6 V) applied to the needles for 30 s. If VF spontaneously reverted to sinus rhythm, the stimulation was repeated. VF was confirmed when arterial pulsation disappeared, the blood pressure dropped rapidly to <20 mmHg, and the electrocardiogram displayed VF waveforms. CPR was begun at 7 min VF by administering chest compressions, which was performed by chest compression device at a frequency of 200/min, and a depth of 1/3 the anteroposterior thoracic diameter. Mechanical ventilation was also given at a rate of 75 times/min, and the parameters of the ventilator were adjusted to maintain arterial PCO_2 at 35–45 mmHg. If spontaneous circulation did not recover after 2 min, CPR was continued, and 20 $\mu\text{g}/\text{kg}$ epinephrine boluses were injected every 3 min until ROSC, defined as mean arterial pressure (MAP) >60 mmHg for at least 10 min. Resuscitation efforts were abandoned if ROSC was not achieved after 20 min CPR.

Echocardiography

Cardiac ultrasound was performed before VF and 4 h after ROSC. The probe was placed on the left side of the sternum, and longitudinal and transverse parasternal and 4- and

2-chamber apical views were obtained. Left ventricular M-mode measurements at the level of the papillary muscles were used to estimate Ejection Fraction (EF).¹⁴ The average of three EF measurements per animal was used for analysis.

Experiment 1. Observing the effect of HPC on rat's heart function and 72 h survival status after ROSC

Thirty-six Wistar rats were randomly divided into three groups. The Control group had a normal temperature maintained throughout the experiment. If necessary, an electric blanket was used to keep the rectal temperature at $37 \pm 0.5^\circ\text{C}$. The animals in the HPC group were cooled to $32\text{--}34^\circ\text{C}$ for half an hour by an ice blanket before inducing VF. In the HPC + Compound C group, Compound C (10 mg/kg) was administered i.p. 30 min before initiating HPC. After ROSC, the temperature in both HPC groups was increased at 0.5°C per hour, achieving normothermia within 4–6 h. The hemodynamic parameters, echocardiogram data, and survival status of rats were recorded. Supplementary Figure 1 summarized the study design.

Experiment 2. Effects of HPC on AMPK activity and mitophagy-related gene expression in rat myocardium were evaluated after ROSC for 4 h

Forty-four Wistar rats were randomly divided into four groups: Sham normal temperature group (Sham Control, $n=4$), Sham HPC group (Sham HPC, $n=4$), Control group ($n=12$), HPC group ($n=12$), and HPC + Compound C group ($n=12$). The rats did not undergo VF and CPR, but otherwise underwent the same procedures as did the Control and HPC rats. The rats were sacrificed at 4 h after ROSC. The hearts were excised and washed in 4°C phosphate-buffered saline (PBS), cut into sections for histology at a thickness of 1–2 mm, and frozen in liquid nitrogen for the Western blot to detect the protein expression and real-time polymerase chain reaction (PCR) to quantify the dedicated gene expression.

Experiment 3. Measurement of myocardial autophagic flux

Eighteen rats assigned to Control, HPC, and HPC + Compound C groups (six rats/group) were anesthetized with pentobarbital sodium (30 mg/kg), and mechanically ventilated by tracheal intubation. The heart was exposed by left thoracotomy, and then $50\ \mu\text{L}$ AAV9-mRFP-GFP-LC3 was injected directly into the pericardial cavity through the left ventricular free wall (LC3 virus concentration 3×10^{13} , Hanbio Co. Ltd., Shanghai, China). Then, the chest wall was sutured closed, and the animal was extubated after awakening from anesthesia and returned to its cage. Two weeks later, the rats underwent the VF-CPR-ROSC protocol described above. Likewise, and the hearts were collected 4 h after ROSC. The long axis section of the LV was identified by fluorescent staining. Images were taken under confocal microscope (Olympus, Tokyo, Japan). The red LC3 puncta were manually counted.

Isolation and culture of neonatal rat CMs

Culture plates were coated with $40\ \mu\text{g}/\text{mL}$ poly-D-lysine (PDL) (Sigma, P6407). The heart was taken from a one-day

old Sprague Dawley (SD) rat after hypothermic anesthesia. The heart was placed in a 10-cm petri dish filled with low-temperature D-Hanks solution. The LV and a small amount of right ventricle were isolated and cut into $0.5\ \text{mm}^3$ pieces which were digested in 0.25% Trypsin-EDTA (Gibco, 930004) for 30 min at 37°C to isolate individual CMs. CMs were layered on PDL-coated plates for 5 h in Dulbecco's Modified Eagle Medium (DMEM) high glucose medium (Gibco, 11960085) supplemented with 5% fetal bovine serum (FBS, Gibco, 1581729) and 1% penicillin/streptomycin (Hyclone, SV30010). Twelve hours later, the medium was changed with culture medium containing $0.1\ \text{mmol}/\text{L}$ Bromodeoxyuridine (BrdU, Sigma) for 24 h to inhibit fibroblast growth, and then the medium was replaced with fresh culture medium.

Adenoviral infection of CMs

Three days after plating, cells were infected with adenovirus expressing RFP-GFP-LC3 (multiplicity of infection, MOI = 10) for 48 h. Plates were then assigned randomly to six groups: (1) normal CMs, maintained at 37°C (NC + Control); (2) normal HPC group (NC + HPC), CMs were incubated at 33°C for 30 min and then returned to 37°C for cultivation; (3) normal CMs combined with $2\ \mu\text{mol}/\text{L}$ of Compound C followed by HPC (NC + HPC + Compound C); (4) Control + I6R4: after the medium was replaced with hypoxia solution, plates were kept in a hypoxia chamber ($<5\% \text{O}_2$) for 6 h as described below, then the medium was replaced with the complete medium and the plates were maintained under $21\% \text{O}_2$ at 37°C for 4 h again; (5) HPC + I6R4: the CMs underwent 6 h hypoxia + 4 h reperfusion after HPC; (6) HPC + Compound C + I6R4: CMs underwent HPC after Compound C was added to medium at $2\ \mu\text{mol}/\text{L}$, and then underwent I/R.

To produce simulated ischemia, the CMs were rinsed twice and then bathed in anoxic medium containing ($20\ \text{mmol}/\text{L}$ Deoxyglucose, $10.2\ \text{mmol}/\text{L}$ KCl, $1.2\ \text{mmol}/\text{L}$ MgSO_4 , $6.3\ \text{mmol}/\text{L}$ NaHCO_3 , $20\ \text{mmol}/\text{L}$ HEPES, $125\ \text{mmol}/\text{L}$ NaCl, $1.2\ \text{mmol}/\text{L}$ KH_2PO_4 , $1.2\ \text{mmol}/\text{L}$ CaCl_2 , and $5\ \text{mmol}/\text{L}$ sodium lactate, pH 6.6). Cell culture plates were arranged into a modular chamber (CA92014, Billups-Rothenberg, San Diego, CA, USA) with a closing hose. To impose hypoxia, gas containing $95\% \text{N}_2$ and $5\% \text{CO}_2$ was continuously pumped ($0.2\ \text{L}/\text{min}$) into the chamber. The ventilation pipe was closed 5 min after the atmosphere stabilized at $0.3\% \text{O}_2$ (O_2 sensor: SMART SENSOR, AS8801) 0.3% .

Western blot procedure

Samples were lysed in ice-cold 98% RIPA (Beyotime, Shanghai, China; P0013B), 1% phenylmethanesulfonyl fluoride (PMSF, Beyotime, ST506), and 1.0% protease/phosphatase inhibitor (PI/PHI; Thermo Scientific, Waltham, MA, USA; 78440). Protein concentrations were determined using a Pierce BCA Protein Assay Kit (Beyotime, P0009). $20\ \mu\text{g}$ of total protein per lane was resolved by 10% sodium dodecyl-sulfate polyacrylamide gel electrophoresis (SDS-PAGE) using Mini-PROTEAN® Tetra Cell (Bio-Rad, Hercules, CA, USA; 1658001EDU) and transferred onto $0.2\ \mu\text{m}$ polyvinylidene fluoride (PVDF) membranes (Millipore, Burlington, MA, USA; ISEQ00010) using 2-Gel Tetra and Blotting Module (Bio-Rad, 1660827EDU). The membranes were subsequently

Table 1. Resuscitation parameters of rats between three groups.

	Control (n = 12)	HPC (n = 12)	HPC + Compound C (n = 12)
	Median (minimum, maximum)	Median (minimum, maximum)	Median (minimum, maximum)
Body weight (g)	390 (350, 416)	390 (365, 410)	395 (355, 420)
Temperature (°C)	37 (36, 38.8)	37 (36, 38.7)	36.9 (36, 38.5)
Epinephrine (μg)	38 (0, 744)	16 (0, 222)*†	45 (32, 812)
Countershocks	2 (0, 9)	1 (0, 5)*†	2 (0, 8)
Basic life support (min)	4.2 (3.2, 5.4)	1.8 (1.6, 3.2)**	3.6 (3.1, 6.1)
ROSC rate	6/12	10/12	7/12

Control: normothermia group; HPC: hypothermia preconditioning group; HPC + Compound C: hypothermia preconditioning + Compound C group; ROSC: return of spontaneous circulation.

Values are reported as median (minimum, maximum).

* $P < 0.05$ versus Control; † $P < 0.05$ versus HPC + Compound C.

blocked with 5% bovine serum albumin (BSA, Sigma, A7030) at room temperature for 1 h and incubated with the primary antibodies at 4°C overnight. Afterwards, the membranes were incubated with secondary polyclonal antibodies (horseradish peroxidase (HRP)-labeled goat antirabbit IgG) for 1 h at room temperature. The membranes were exposed to Immobilon Western Chemiluminescent HRP Substrate and evaluated using the chemiluminescent imaging analysis system (General Electric, Boston, MA, USA; ImageQuant Las4000mini).

Reverse transcription-quantitative polymerase chain reaction detection of relative abundances of mRNA transcripts

Samples were lysed using Trizol (Invitrogen, Waltham, MA, USA; 15596026) at room temperature for 5 min. Trizol containing 200 mmol/L chloroform was added and shaken vigorously for 15 s. After 2 min, the mixture was centrifuged at 10,624g at 4°C for 15 min. The upper aqueous phase including total RNA was collected, mixed with equal isopropanol for 10 min, and centrifuged at 10,624g at 4°C for 15 min. The supernatant was discarded. Appropriate 1 mL 75% alcohol was added and centrifuged at 10,624g at 4°C for 10 min. The supernatant was removed, and then the concentration of total RNA was measured. For each sample, 1 μg total RNA was reverse transcribed into cDNA using the PrimeScript™ RT reagent Kit with gDNA Eraser (Takara, Kusatsu, Shiga, Japan; RR047A). Relative gene transcription was measured by SYBR® Premix Ex Taq™ II (Takara, RR820A). Reverse transcription-quantitative polymerase chain reaction (RT-qPCR) was executed in a Real-Time PCR System (Bio-Rad, CFX96 touch). In every RT-qPCR test, met curves were detected at the end of the experiment to examine primer specificity. Relative mRNA transcription was normalized to β-actin and counted using the $F = 2^{(-\Delta\Delta Ct)}$ formula. Gene-specific primers were synthesized by Invitrogen. Primer sequences are provided in Supplementary Data 2.

Statistics

Data are presented as median (minimum, maximum). Normally distributed data were analyzed with parametric tests. Group values were compared by one-way analysis of variance (ANOVA), followed by the Bonferroni test for multiple comparisons. Non-normal data were analyzed with

non-parametric tests (the Kruskal–Wallis test for ≥ 3 groups followed by the Dunn test to correct for multiple comparisons). Hemodynamic values at different time points between the groups were compared using two-way repeated-measures analysis of variance. The Fisher exact test was used to compare the ROSC rate between groups. The Kaplan–Meier survival curve analysis and the log-rank test were used for comparisons of survival between groups. The statistical significance was assumed at P -values < 0.05 . All statistical analyses were performed using the SPSS 22.0 software (IBM Corp., Armonk, NY, USA).

Results

CPR parameters

There were no statistically significant differences in body weight, temperature, and EF among the Control, HPC and HPC + Compound C groups at baseline (Table 1). Six of 12 rats in the Control group, 10 of 12 rats in the HPC group, and 7 of 12 rats in the HPC + Compound C achieved ROSC. Although the recovery frequencies did not differ significantly, a trend toward increased ROSC in the HPC group versus the Control and HPC + Compound C groups was achieved. During resuscitation, the number of countershocks required to achieve defibrillation in the HPC group was significantly less than in the Control and HPC + Compound C groups ($P = 0.002$ vs Control, $P = 0.02$ vs HPC + Compound C). The amount of epinephrine used was also the lowest in HPC group ($P = 0.001$) (Table 1).

HPC improved cardiac contractility and promoted survival rate of rats after ROSC

The LVESP and dp/dt_{max} reflect the left ventricular systolic function, and the LVEDP and dp/dt_{min} represent the left ventricular diastolic function. After ROSC, cardiac function was impaired in all three groups, but LVESP and dp/dt_{max} stabilized at high levels in HPC group would rise incrementally over time, and sustain for a 4-h period compared with the Control and HPC + Compound C groups (Figure 1(A) and (B)). Diastolic function was similarly impaired in all three groups after ROSC (Figure 1(C) and (D)).

CO and EF also were evaluated to further assess the impact of HPC ± Compound C on postarrest cardiac

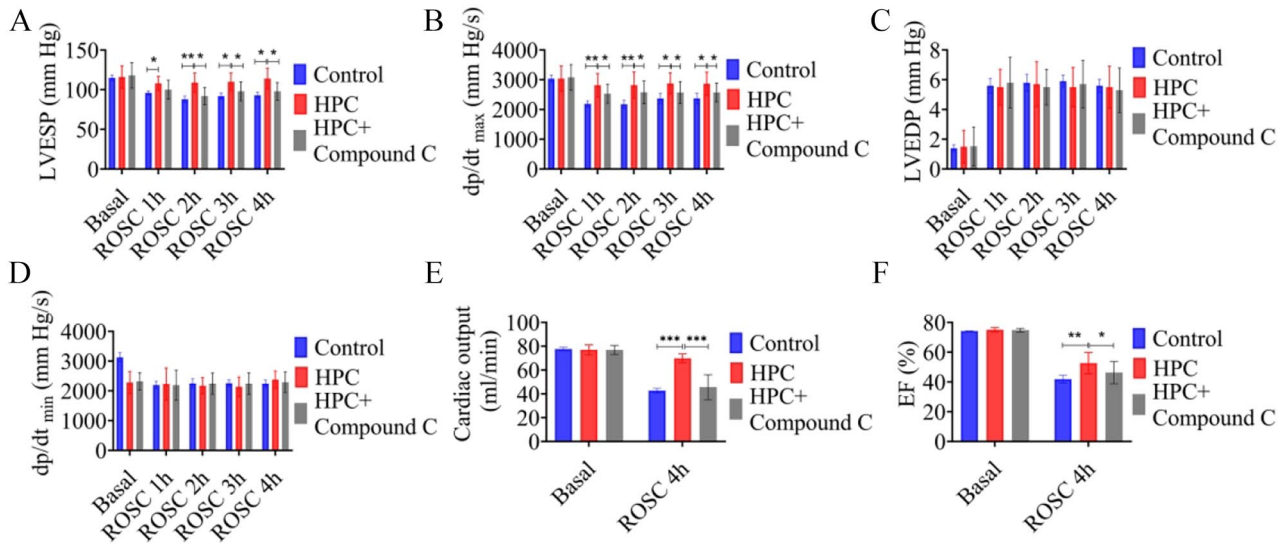


Figure 1. HPC improved rat cardiac contractile function and promoted survival rate after ROSC: The LVESP and dp/dt_{max} (A and B) after ROSC were impaired in all groups ($P < 0.01$). Contractile function improved in HPC group at 1 h after ROSC and can be sustained for 4 h, whereas diastolic function was not affected by HPC (C and D). Four hours after ROSC, the CO in the Control group was significantly lower than HPC and HPC + Compound C groups (E). EF measured by echocardiography showed HPC preserved better cardiac function (F). (A color version of this figure is available in the online journal.)
* $P < 0.05$; ** $P < 0.01$; *** $P < 0.001$.

function. Pre-VF baseline CO and EF were approximately 77 ± 3 mL/min and $75 \pm 1\%$, respectively, in all three groups (Figure 1(E) and (F)), indicating that neither HPC nor Compound C pretreatment affected cardiac function before VF. However, the treatment effects on CO and EF emerged after ROSC. At 4 h after ROSC, CO in the Control group declined to 43 ± 5 mL/min, while in the HPC group, CO was stabilizing at 70 ± 4 mL/min. Compound C abrogated the HPC-induced improvement in CO (45 ± 15 mL/min; $P < 0.01$) (Figure 1(E)). EF at 4 h ROSC showed similar treatment effect: $42 \pm 4\%$ in the Control group, $59 \pm 3\%$ in the HPC group, and 46.3 ± 7 in the HPC + Compound C group ($P = 0.001$) (Figure 1(F)).

Six HPC rats, but only one Control rat and two HPC + Compound C rats survived 72 h. The Post-ROSC Kaplan–Meier survival analysis showed that HPC improved the survival rate (Figure 2).

HPC activated the myocardial AMPK-ULK1-mitophagy pathway

HPC increased myocardial AMPK α and ULK1 phosphorylation in the Sham and CPR groups in comparison with other groups, but did not affect Akt phosphorylation (Figure 3(A) to (D)). Meanwhile, the protein contents of the essential autophagy elements ATG7, ATG5, and LC3-II increased significantly in myocardium of HPC-created rats, both before and after VF-CPR-ROSC (Figure 3(E) to (G)).

To further evaluate the activation of autophagy, we examined the immunofluorescence of microtubule associated protein 1 LC3 in myocardium. AAV9-mRFP-GFP-LC3 was used to measure the autophagic flux in myocardium. We found that most of myocardium was infected after injection of AAV9-mRFP-GFP-LC3 for two weeks. HPC significantly increased the number of RFP-LC3 particles in the myocardium at 4 h after ROSC (Figure 4(A) and (B)).

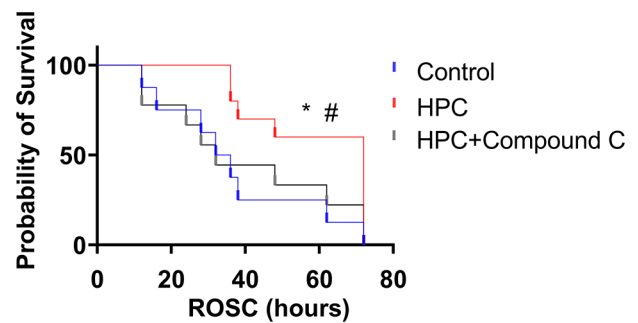


Figure 2. Cumulative survival in the three groups. HPC improved the survival rate of rats after ROSC at 72 h. (A color version of this figure is available in the online journal.)
* $P < 0.05$ versus Control; # $P < 0.05$ versus HPC + Compound C.

Our previous research demonstrated that HPC can improve myocardial mitochondrial function.¹⁰ Given that mitophagy plays a central role in mitochondrial quality control, we investigated if HPC promoted mitochondrial autophagy¹⁵ by performing quantitative polymerase chain reaction (qPCR) for mRNA quantification of genes involved in mitophagy. qPCR indicated that HPC promoted the expression of mitophagy-related genes at 4 h after ROSC, including *Bnip1*, *Bnip3L*, *Parkin*, *Pink1*, *Sqstm1*, and *Ulk1*, but Compound C decreased expression of all six of these genes (Figure 4(C) to (H)). These results confirmed that mitochondrial autophagy was involved in the protective effect of HPC on the myocardium after ROSC, Compound C blocked HPC induction of mitophagy.

HPC promoted the survival of CMs after I/R by activating AMPK *in vitro*

In vitro, the survival of CMs under HPC-treated exceeded than the CMs in the control group (70.1% vs 48.6% , $P < 0.001$)

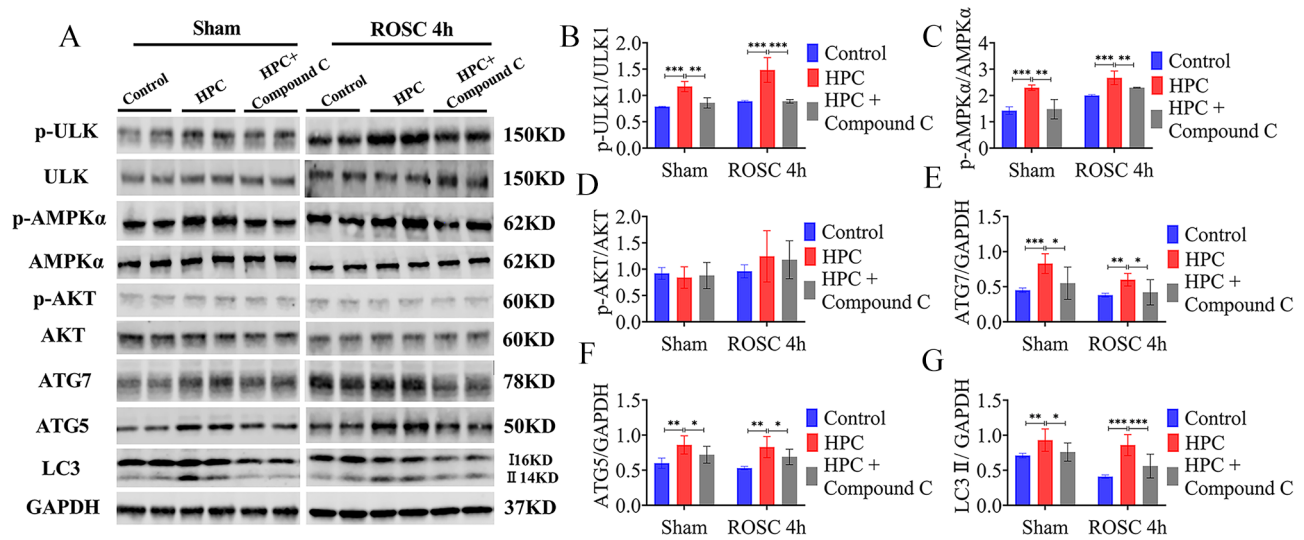


Figure 3. HPC-activated AMPK-ULK1-mitophagy pathway in myocardium: HPC increased the levels of p-AMPK α and p-ULK1 in the myocardium, but the level of p-Akt did not change (A to D). The protein levels of ATG7, ATG5, and LC3-II increased significantly (E to G). Compound C compromised the activation of mitophagy genes expression. (A color version of this figure is available in the online journal.)
* $P < 0.05$; ** $P < 0.01$; *** $P < 0.001$.

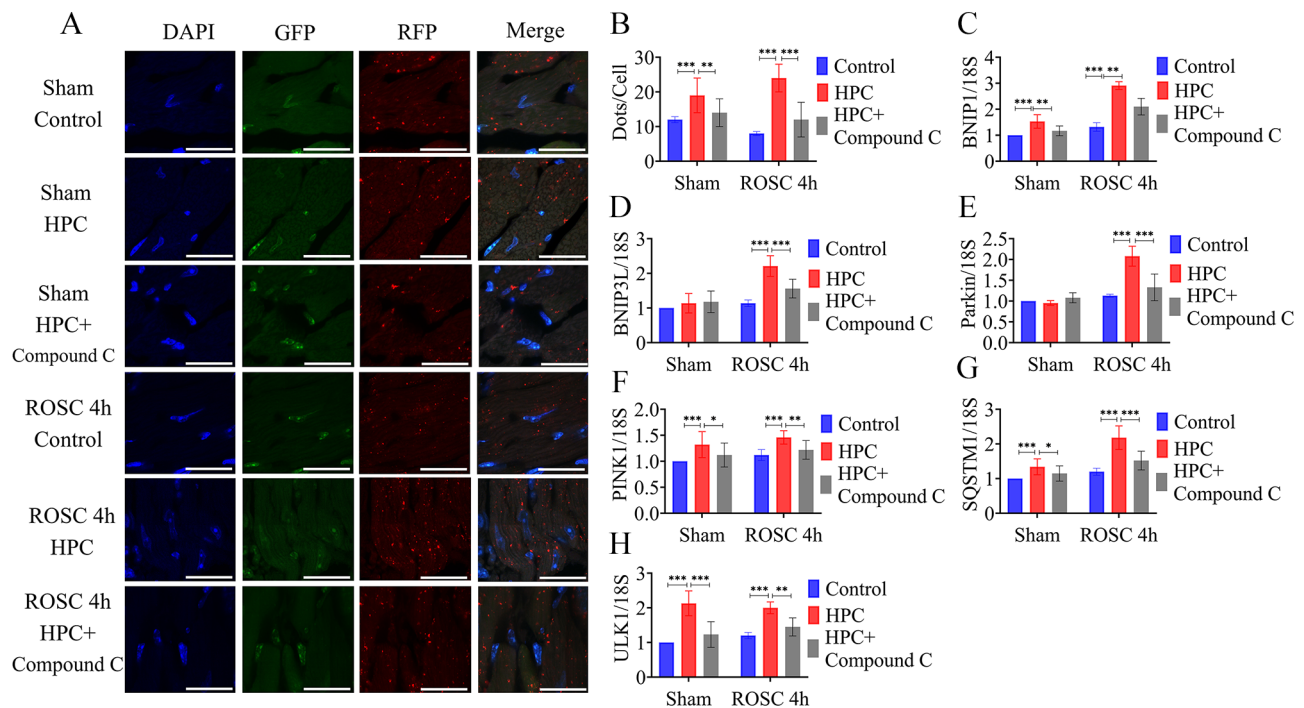


Figure 4. HPC promoted mitochondrial autophagy in myocardium: the number of RFP-LC3 particles in myocardium increased exposed to the Sham + HPC group and HPC group after ROSC for 4h, Compound C compromised the autophagic Flux (A and B, scale bars 25 μ m). HPC promoted the expression of mitochondrial autophagy-related genes, *Bnip1*, *Bnip3L*, *Parkin*, *Pink1*, *Sqstm1*, and *Ulk1* at 4h after ROSC (C to H). (A color version of this figure is available in the online journal.)
* $P < 0.05$; ** $P < 0.01$; *** $P < 0.001$.

after I/R. The AMPK inhibitor Compound C¹⁶ attenuated the protective effect of HPC, lowering CMs survival to 57.5% (Figure 5(A) and (B)). Moreover, HPC significantly increased AMPK and ULK1 phosphorylation and LC3-II content for at least 4h after hypoxia-reoxygenation, and Compound C yet again blunted these HPC effects (Figure 5(C) to (F)).

In CMs, consistent with the observations obtained from the *in vivo* experiments, HPC treatment activated expression

of mitochondrial autophagy-related genes and increased autophagic flux at 4h after hypoxia-reoxygenation (Figure 6(A) to (H)).

Again, the AMPK inhibitor, Compound C blocked HPC's activation of AMPK-ULK1-mitophagy pathway, blunted the expression of mitophagy-related genes, and reduced autophagic flux in CMs, thus weakening HPC of CMs subjected to simulated I/R (Figure 6(A) to (H)). Collectively,

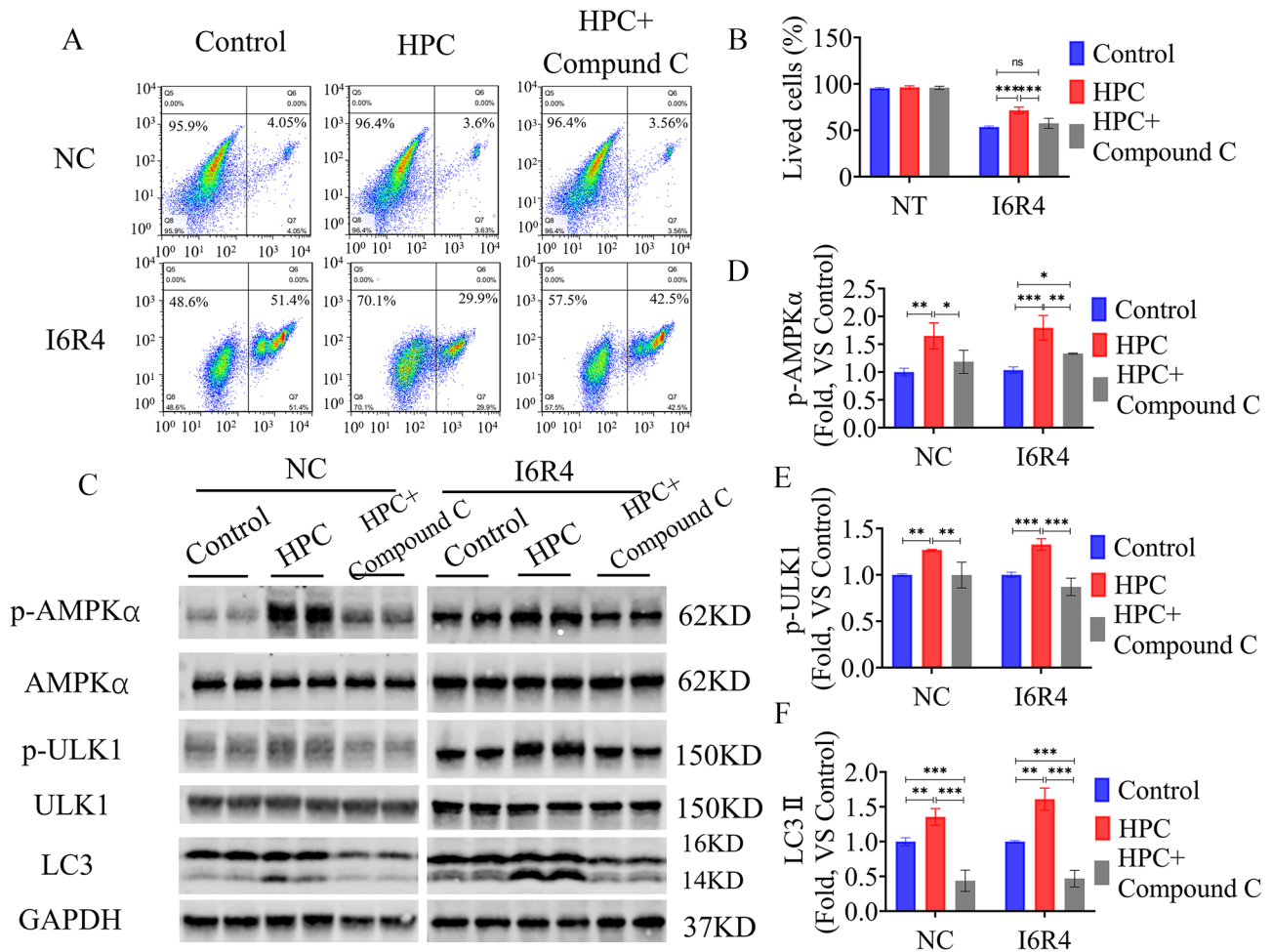


Figure 5. HPC promoted the survival of CMs after I/R induced by AMPK-ULK1 mitophagy: the survival rate of CMs in HPC group was higher than the Control group, whereas the protection was compromised by Compound C (A and B). Furthermore, the protein levels of p-AMPK, ULK1, and LC3-II increased significantly in the HPC group, and down-regulated by Compound C (C to F). (A color version of this figure is available in the online journal.)

NC: normothermia control.

* $P < 0.05$; ** $P < 0.01$; *** $P < 0.001$.

these findings suggested HPC activated the AMPK-ULK1-mitophagy pathway in CMs.

Discussion

This study investigated the mechanisms leading to the cardiac protection of HPC. The major findings from this study suggest that (1) HPC significantly increased survival of rats after CA/CPR and promoted survival of CMs after I/R, (2) HPC increased AMPK activity, expression of autophagy-related protein LC3-II and mitophagy genes, and autophagic flux both *in vivo* and *in vitro*, (3) Compound C, which as expected blocked AMPK in cultured CM, attenuated HPC-induced cardioprotection, and inhibited autophagy induced by HPC. To the best of our knowledge, this is the first study that demonstrates AMPK-induced mitophagy plays an important role in the cardioprotection by HPC after CA.

Mitochondria are major targets in I/R injury and their dysfunction plays a crucial role in cardiovascular disease pathogenesis.^{9,17,18} The selective removal of damaged mitochondria by mitophagy is regarded as a critical protective mechanism against I/R injury in the heart, and the inhibition

of mitophagy promotes mitochondrial dysfunction and cardiac dysfunction.^{19,20} In this study, mitophagy increased significantly in HPC-pretreated myocardium at 4h after ROSC, and HPC increased autophagic flux and mitophagy gene expression in CMs. These findings are consistent with previous studies showing that hypothermia enhances mitophagy and improves I/R injury.^{21,22} Noticeably, although mitophagy induction has been identified as a key component in HPC protection of ischemic heart, the benefit may be attenuated by excessive mitophagy. Studies demonstrated that excessive autophagy and mitophagy worsen mitochondria quality, which increases the severity of postresuscitation myocardial dysfunction and aggravates brain damage after CA.²³⁻²⁵ These studies raise a thought-provoking question as to how much mitophagy is optimal to elicit a maximum amount of tolerance during I/R. Interestingly, some studies have found that hypoxia can upregulate mitophagy,^{19,26} while the extent of mitophagy of hypoxia myocardium is not enough to improve cardiac function. In this study, 30 min of hypothermia prior to ischemia resulted in a higher level of mitophagy in the early phase after ROSC and resulted in improved cardioprotection after CA.

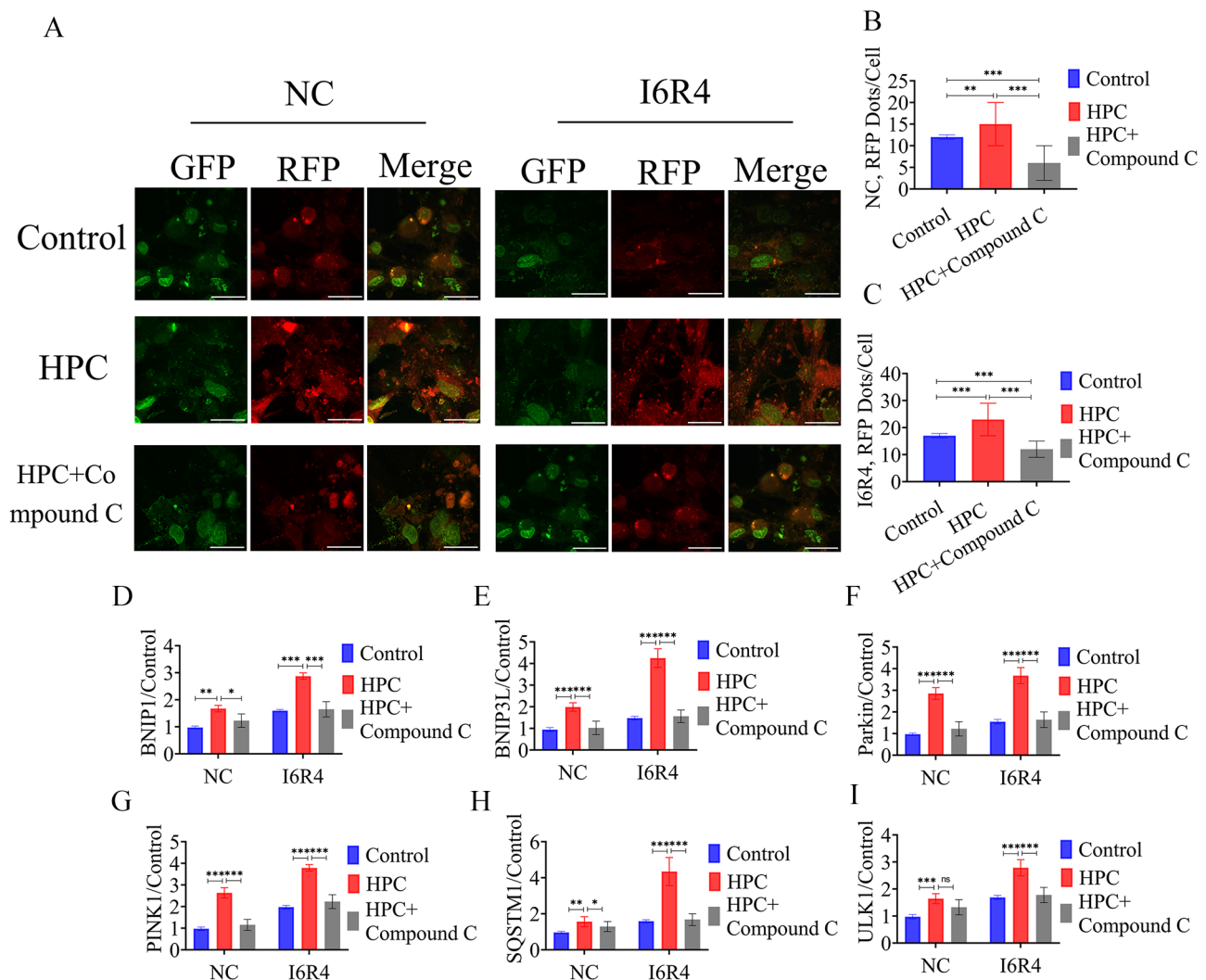


Figure 6. HPC activated the AMPK-ULK1-mitophagy pathway in cardiomyocytes: the autophagic flux was activated in HPC group and weakened by Compound C after I/R. Compared to NC group, the number of RFP-LC3 particles in cardiomyocytes was increased exposed to the HPC group, and decreased in HPC + Compound C group (A and B, scale bars 25 μ m). Moreover, the expression of mitochondrial autophagy-related genes and ULK1 (C to H) increased under HPC, and reduced by Compound C after I/R. (A color version of this figure is available in the online journal.)

NC: normal control.

* $P < 0.05$; ** $P < 0.01$; *** $P < 0.001$.

Another important outcome of this study is that we verified that HPC-induced mitophagy by activating AMPK. AMPK activation can protect CMs and limit the damage from myocardial ischemic injury by activation of glucose uptake and glycolysis during ischemia and limiting apoptotic activity associated during reperfusion.²⁷ Evidence also shows that AMPK serves a critical role in enhancing mitophagy by phosphorylation of ULK1 or PINK1.^{28,29} In this study, AMPK and ULK1 protein phosphorylation and mitophagy gene expression increased significantly after 4h of reperfusion both *in vivo* and *in vitro*, accompanied by increased autophagic flux in HPC group. To further interrogate the role of AMPK in regulating the mitophagy-inducing effects of HPC, experiments should be conducted with the AMPK inhibitor Compound C. We found Compound C suppressed HPC-induced mitophagy and undermined the effects of HPC on CMs after I/R. Our findings demonstrate that AMPK-activated mitophagy is critically involved in HPC-induced cardioprotection. This outcome is concordance with

our previous findings that mitochondrial function and adenosine triphosphate (ATP) levels are conserved with HPC.¹⁰

In this study, we demonstrated that administrating 30 min of hypothermia before ischemia could mitigate cardiac contractility dysfunction and hemodynamic impairment by improving EF, CO, and left ventricular systolic function follow ROSC. However, HPC did not improve diastolic function. Currently, the impact of hypothermia therapy on cardiac function after CA is still controversial.³⁻⁵ Animal studies have demonstrated that hypothermia worsens diastolic function by prolonging LV relaxation and reducing LV end diastolic capacitance.^{6,7} In this study, HPC did not affect or worsen diastolic function after ROSC compared to Control group. The difference can be attributed to the timing and duration of hypothermia strategy. Of note, in this study, cooling improved inotropy and CO, which enhanced the survival of rats *in vivo* and CMs *in vitro*.

This study has several limitations. First, we did not evaluate LV performance and mitochondrial function after 4h,

where the full recovery of cardiac function can be observed. The early recovery of cardiac function after CA is related to an important predictor of survival rate.^{2,30} Although we only studied cardiac function during the early phases of postarrest recovery, it is likely that prolonging observation time may clarify the process of the recovery of diastolic function and full recovery of systolic function. Second, we utilized mitophagy-related gene expression and fluorescence detection of autophagic flux to represent the complex process of mitophagy instead of directly accessing mitochondrial fluorescence. Still, it is well documented that mitophagy can be regulated by AMPK through ULK1, so our result is adequate to address our hypothesis.^{12,29,31,32}

In conclusion, this study demonstrates that HPC improves postresuscitation cardiac contractility by promoting mitophagy activated by the AMPK pathway. Currently, HPC is used most commonly to extend the brain's tolerance to ischemic damage and attenuate brain injury in neurosurgery and cardiovascular surgery. Further elucidation of the cardioprotection mechanisms of HPC is essential to support its potential clinical use in patients who are at high risk of CA.

AUTHORS' CONTRIBUTIONS

All the co-authors have made contributions to this study and approved the version to be published. Y.L. and C.Z. both are responsible for the acquisition and analysis of the data, and drafting of the manuscript. C.H. and X.L. designed the study, interpreted the data, and revised the manuscript. M.P.C. analyzed data and revised manuscript. The rest of the co-authors participated in the animal experiments, data collection, laboratory tests, and revision of the manuscript.

DECLARATION OF CONFLICTING INTERESTS

The author(s) declared no potential conflicts of interest with respect to the research, authorship, and/or publication of this article.

FUNDING

The author(s) disclosed receipt of the following financial support for the research, authorship, and/or publication of this article: This study was supported by funding from the National Nature Science Foundation of China (grant nos 81571867 and 81901931), the Science and Technology Project of Shenzhen city of China (grant no. JCYJ20160608142215491); the Guangdong Basic and Applied Basic Research Foundation (grant nos 2020A1515010120, 2020A1515110919, and 2020A1515110827); the Shenzhen Fundamental Research Program (grant no. JCYJ20190809150817414). The funders had no role in the study design, data collection, analysis, decision to publish, or preparation of the manuscript.

ORCID ID

Chunlin Hu  <https://orcid.org/0000-0002-9510-0957>

SUPPLEMENTAL MATERIAL

Supplemental material for this article is available online.

REFERENCES

- Laver S, Farrow C, Turner D, Nolan J. Mode of death after admission to an intensive care unit following cardiac arrest. *Intens Care Med* 2004; 30:2126–8
- Laurent I, Monchi M, Chiche JD, Joly LM, Spaulding C, Bourgeois B, Cariou A, Rozenberg A, Carli P, Weber S, Dhainaut JF. Reversible myocardial dysfunction in survivors of out-of-hospital cardiac arrest. *J Am Coll Cardiol* 2002;40:2110–6
- Arrich J. Clinical application of mild therapeutic hypothermia after cardiac arrest. *Crit Care Med* 2007;35:1041–7
- Hsu CY, Huang CH, Chang WT, Chen HW, Cheng HJ, Tsai MS, Wang TD, Yen ZS, Lee CC, Chen SC, Chen WJ. Cardioprotective effect of therapeutic hypothermia for postresuscitation myocardial dysfunction. *Shock* 2009;32:210–6
- Stegman B, Aggarwal B, Senapati A, Shao M, Menon V. Serial hemodynamic measurements in post-cardiac arrest cardiogenic shock treated with therapeutic hypothermia. *Eur Heart J Acute Cardiovasc Care* 2015;4:263–9
- Post H, Schmitto JD, Steendijk P, Christoph J, Holland R, Wachter R, Schondube FW, Pieske B. Cardiac function during mild hypothermia in pigs: increased inotropy at the expense of diastolic dysfunction. *Acta Physiol* 2010;199:43–52
- Schwarzl M, Alogna A, Zirngast B, Steendijk P, Verderber J, Zweiker D, Huber S, Maechler H, Pieske BM, Post H. Mild hypothermia induces incomplete left ventricular relaxation despite spontaneous bradycardia in pigs. *Acta Physiol* 2015;213:653–63
- Sciarretta S, Maejima Y, Zablocki D, Sadoshima J. The role of autophagy in the heart. *Annu Rev Physiol* 2018;80:1–26
- Chistiakov DA, Shkurat TP, Melnichenko AA, Grechko AV, Orekhov AN. The role of mitochondrial dysfunction in cardiovascular disease: a brief review. *Ann Med* 2018;50:121–7
- Lu Y, Zeng X, Jing X, Yin M, Chang MMP, Wei H, Yang Y, Liao X, Dai G, Hu C. Pre-arrest hypothermia improved cardiac function of rats by ameliorating the myocardial mitochondrial injury after cardiac arrest. *Exp Biol Med* 2019;244:1186–92
- Salt IP, Hardie DG. AMP-activated protein kinase: an ubiquitous signaling pathway with key roles in the cardiovascular system. *Circ Res* 2017;120:1825–41
- Tian W, Li W, Chen Y, Yan Z, Huang X, Zhuang H, Zhong W, Chen Y, Wu W, Lin C, Chen H, Hou X, Zhang L, Sui S, Zhao B, Hu Z, Li L, Feng D. Phosphorylation of ULK1 by AMPK regulates translocation of ULK1 to mitochondria and mitophagy. *FEBS Lett* 2015;589:1847–54
- Li X, Liu YJ, Xia JM, Zeng XY, Liao XX, Wei HY, Hu CL, Jing XL, Dai G. Activation of autophagy improved the neurologic outcome after cardiopulmonary resuscitation in rats. *Am J Emerg Med* 2016;34:1511–8
- Watson LE, Sheth M, Denyer RF, Dostal DE. Baseline echocardiographic values for adult male rats. *J Am Soc Echocardiogr* 2004;17:161–7
- Saito T, Sadoshima J. Molecular Mechanisms of Mitochondrial Autophagy/Mitophagy in the Heart. *CIRC RES* 2015;116:1477–90
- Dasgupta B, Seibel W. Compound C/dorsomorphin: its use and misuse as an AMPK inhibitor. *Methods Mol Biol* 2018;1732:195–202
- Disatnik MH, Hwang S, Ferreira JC, Mochly-Rosen D. New therapeutics to modulate mitochondrial dynamics and mitophagy in cardiac diseases. *J Mol Med* 2015;93:279–87
- Siasos G, Tsigkou V, Kosmopoulos M, Theodosiadis D, Simantiris S, Tagkou NM, Tsimipiktsioglou A, Stampoulou PK, Oikonomou E, Mourouzis K, Philippou A, Vavuranakis M, Stefanadis C, Tousoulis D, Papavassiliou AG. Mitochondria and cardiovascular diseases—from pathophysiology to treatment. *Ann Transl Med* 2018;6:256
- Zhang W, Ren H, Xu C, Zhu C, Wu H, Liu D, Wang J, Liu L, Li W, Ma Q, Du L, Zheng M, Zhang C, Liu J, Chen Q. Hypoxic mitophagy regulates mitochondrial quality and platelet activation and determines severity of I/R heart injury. *Elife* 2016;5:e21407
- Hoshino A, Mita Y, Okawa Y, Ariyoshi M, Iwai-Kanai E, Ueyama T, Ikeda K, Ogata T, Matoba S. Cytosolic p53 inhibits Parkin-mediated mitophagy and promotes mitochondrial dysfunction in the mouse heart. *Nat Commun* 2013;4:2308
- Marek-Iannucci S, Thomas A, Hou J, Crupi A, Sin J, Taylor DJ, Czer LS, Esmailian F, Mentzer RM Jr, Andres AM, Gottlieb RA. Myocardial hypothermia increases autophagic flux, mitochondrial mass and myocardial function after ischemia-reperfusion injury. *Sci Rep* 2019;9:10001

22. Zhou T, Liang L, Liang Y, Yu T, Zeng C, Jiang L. Mild hypothermia protects hippocampal neurons against oxygen-glucose deprivation/reperfusion-induced injury by improving lysosomal function and autophagic flux. *Exp Cell Res* 2017;**358**:147–60
23. Lu J, Qian HY, Liu LJ, Zhou BC, Xiao Y, Mao JN, An GY, Rui MZ, Wang T, Zhu CL. Mild hypothermia alleviates excessive autophagy and mitophagy in a rat model of asphyxial cardiac arrest. *Neurol Sci* 2014;**35**:1691–9
24. Lu J, Shen Y, Liu LJ, Qian HY, Zhu CL. Combining epinephrine and esmolol attenuates excessive autophagy and mitophagy in rat cardiomyocytes after cardiac arrest. *J Cardiovasc Pharmacol* 2015;**66**:449–56
25. Huang Y, Gao X, Zhou X, Xie B, Zhang Y, Zhu J, Zhu S. Mitophagy in the hippocampus is excessive activated after cardiac arrest and cardiopulmonary resuscitation. *Neurochem Res* 2020;**45**:322–30
26. Zhang H, Liu B, Li T, Zhu Y, Luo G, Jiang Y, Tang F, Jian Z, Xiao Y. AMPK activation serves a critical role in mitochondria quality control via modulating mitophagy in the heart under chronic hypoxia. *Int J Mol Med* 2018;**41**:69–76
27. Russell RR 3rd, Li J, Coven DL, Pypaert M, Zechner C, Palmeri M, Giordano FJ, Mu J, Birnbaum MJ, Young LH. AMP-activated protein kinase mediates ischemic glucose uptake and prevents postischemic cardiac dysfunction, apoptosis, and injury. *J Clin Invest* 2004;**114**:495–503
28. Egan DF, Shackelford DB, Mihaylova MM, Gelino S, Kohnz RA, Mair W, Vasquez DS, Joshi A, Gwinn DM, Taylor R, Asara JM, Fitzpatrick J, Dillin A, Viollet B, Kundu M, Hansen M, Shaw RJ. Phosphorylation of ULK1 (hATG1) by AMP-activated protein kinase connects energy sensing to mitophagy. *Science* 2011;**331**:456–61
29. Wang B, Nie J, Wu L, Hu Y, Wen Z, Dong L, Zou MH, Chen C, Wang DW. AMPKalpha2 protects against the development of heart failure by enhancing mitophagy via PINK1 phosphorylation. *Circ Res* 2018;**122**:712–29
30. Kern KB, Hilwig RW, Rhee KH, Berg RA. Myocardial dysfunction after resuscitation from cardiac arrest: an example of global myocardial stunning. *J Am Coll Cardiol* 1996;**28**:232–40
31. Bairwa SC, Parajuli N, Dyck JR. The role of AMPK in cardiomyocyte health and survival. *Biochim Biophys Acta* 2016;**1862**:2199–210
32. Hardie DG, Ross FA, Hawley SA. AMPK: a nutrient and energy sensor that maintains energy homeostasis. *Nat Rev Mol Cell Biol* 2012;**13**:251–62

(Received August 12, 2021, Accepted January 28, 2022)